

Calculation of liquid-crystal Frank constants by computer simulation

Michael P. Allen

H. H. Wills Physics Laboratory, Royal Fort, Tyndall Avenue, Bristol BS8 1TL, United Kingdom

Daan Frenkel

Institute for Atomic and Molecular Physics (FOM), P. O. Box 41883, 1009-DB Amsterdam, The Netherlands

(Received 28 September 1987)

We present the first calculations, by computer simulation, of the Frank elastic constants of a liquid crystal composed of freely rotating and translating molecules. Extensive calculations are performed for hard prolate ellipsoids at a single density, and for hard spherocylinders at three densities. For ellipsoids, the resulting Frank constants are of the same order of magnitude as those found experimentally, and in the expected ratios. For spherocylinders, elastic constants increase rapidly with density. Existing density functional theories are only moderately successful in predicting elastic constants.

In recent years, significant progress has been made in the computer simulation of liquid crystals. Monte Carlo simulations have shown that molecules modeled by sufficiently oblate or prolate hard ellipsoids of revolution will form a nematic liquid crystal in addition to a normal fluid.¹⁻³ Systems of oriented spherocylinders exhibit nematic, smectic, and columnar phases,⁴ while spherocylinders with rotational freedom form isotropic, nematic, and smectic fluids.⁵ Recently, molecules interacting through the continuous Gay-Berne-Pechukas ("modified Gaussian overlap")-type of potential have been shown to form a nematic phase.⁶

Clearly, it is currently feasible to simulate equilibrium liquid-crystalline phases for simple model systems. This gives us the opportunity to compute physical properties of liquid crystals that play a central role in theories of the liquid-crystalline state. For example, we recently reported the observation of the divergence of the collective rotation time in the isotropic phase of a system of prolate hard ellipsoids, on approach to the isotropic-nematic transition.⁷ In the present paper, we turn our attention to the nematic phase itself, and report the first measurements by computer simulation of the Frank elastic constants. We examine these quantities for a system of hard ellipsoids at a state point in the nematic region. We also study the nematic phase of a hard spherocylinder system at three different densities: In this case two of the elastic constants are expected to diverge at the nematic-smectic transition.

The first system we have studied consists of 144 hard ellipsoids of revolution, each with a symmetry axis of length $2a$, perpendicular axes of length $2b$, and axial ratio $a/b = 3$. The second system consists of 576 hard spherocylinders of diameter D , distance L between the centers of the spherical caps, and $L/D = 5$. Both systems were enclosed in cuboidal simulation boxes with periodic boundary conditions applied. In both cases we used a collision-by-collision molecular-dynamics simulation method which has been described in earlier work.^{7,8} The molecules are treated as rigid hard bodies of unit mass, with zero moment of inertia about the symmetry axis and perpendicular moments of inertia chosen to be consistent with uni-

form mass distribution through the body. Dynamically, they behave as linear rotors, with the angular velocity always perpendicular to the symmetry axis. Free flight, with constant linear and angular velocities, occurs between impulsive collisions. The collision dynamics are completely determined by conservation of linear and angular momentum and energy, and by the conditions of hardness and smoothness (i.e., the collisional impulse acts along the normal to the surfaces in contact). The program was written to vectorize easily on a CYBER-205 supercomputer. It generated typically 10^6 collisions per hour of central-processing-unit time for the ellipsoid system, and about 3×10^5 collisions per hour for the larger spherocylinder system at the densities studied. Further technical details will be given in a future publication. For the purposes of calculating the static properties investigated here, Monte Carlo simulation would also have been an appropriate method of generating configurations. We note that we have demonstrated directly, by observing molecular diffusion, that all the state points studied here are fluids.

In the following, we measure the degree of nematic ordering by the quantity $S = -2\lambda_0$ where λ_0 is the middle eigenvalue of the ordering matrix \underline{Q} , defined by^{9,10}

$$Q_{\alpha\beta} = \frac{1}{N} \sum_i \frac{3}{2} e_{i\alpha} e_{i\beta} - \frac{1}{2} \delta_{\alpha\beta}, \quad \alpha, \beta = x, y, z. \quad (1)$$

Here, \mathbf{e}_i is a unit vector along the axis of molecule i and $\delta_{\alpha\beta}$ is the Kronecker delta. N is the number of molecules. In a well-defined nematic phase we have $S \approx S' = \lambda_+$, the highest eigenvalue of \underline{Q} ; the choice between S and S' is discussed elsewhere.¹

The Frank elastic constants are defined^{10,11} in terms of the variation of the free-energy density with distortions of the director field $\mathbf{n}(\mathbf{r})$

$$\mathcal{F}(\mathbf{r}) = \frac{1}{2} \{ K_1 (\nabla \cdot \mathbf{n})^2 + K_2 (\mathbf{n} \cdot \nabla \times \mathbf{n})^2 + K_3 [\mathbf{n} \times (\nabla \times \mathbf{n})]^2 \}. \quad (2)$$

K_1 corresponds to splay deformations, K_2 to twist, and K_3 to bend. Explicit ensemble-averaged fluctuation expres-

sions are available for these quantities.¹² These are simply expressed in terms of components of the wave-vector-dependent ordering matrix $\hat{Q}(\mathbf{k})$:

$$\hat{Q}_{\alpha\beta}(\mathbf{k}) = \frac{V}{N} \sum_i \left(\frac{1}{2} e_{i\alpha} e_{i\beta} - \frac{1}{2} \delta_{\alpha\beta} \right) \exp(i\mathbf{k} \cdot \mathbf{r}_i), \quad (3)$$

where \mathbf{r}_i is the position of molecule i and V is the volume. The director $\mathbf{n} = (0,0,1)$ is taken to define the 3-direction in a Cartesian system for a region of the nematic fluid; in a simulation, \mathbf{n} is the eigenvector corresponding to the eigenvalue λ_+ of the ordering matrix of Eq. (1). Taking the wave vector $\mathbf{k} = (k_1, 0, k_3)$ to lie in the 1-3 plane we have¹²

$$E_{13}(k_1^2, k_3^2) \equiv \frac{S^2 V k_B T}{\langle \hat{Q}_{13}(\mathbf{k}) \hat{Q}_{13}(-\mathbf{k}) \rangle} = K_1 k_1^2 + K_3 k_3^2, \quad (4)$$

$$E_{23}(k_1^2, k_3^2) \equiv \frac{S^2 V k_B T}{\langle \hat{Q}_{23}(\mathbf{k}) \hat{Q}_{23}(-\mathbf{k}) \rangle} = K_2 k_1^2 + K_3 k_3^2. \quad (5)$$

In principle, at low k , the simulation-accessible E_{13} and E_{23} should be linear functions of k_1^2 and k_3^2 . In practice, at the values of k accessible in a simulation, higher-order terms may be nonnegligible; nonetheless, a double-polynomial fit to the functions E_{13} and E_{23} , followed by extraction of the coefficients of k_1^2 and k_3^2 at the origin, is a satisfactory route to the elastic constants. In a nematic liquid crystal, all the elastic constants adopt finite values. In a smectic, K_2 and K_3 should be infinite,¹⁰ although it should be borne in mind that Eqs. (4) and (5) only apply in the limit of infinite system size.

Now we turn to the simulations. The ellipsoid system was studied at a single density in the nematic region, $\rho = 0.75\rho_{cp}$ where $\rho_{cp} = \sqrt{2}/8ab^2$ is the close-packed density. This state point was prepared in the following way. A well-equilibrated isotropic fluid system was uniformly compressed during the course of a molecular-dynamics simulation, to a density $\rho = 0.75\rho_{cp}$, well within the nematic region. The pressure of the system rapidly equilibrated at the appropriate value for this density on the nematic branch of the equation of state, as determined by Monte Carlo simulation.³ This took roughly $1400t_c$, where t_c is the mean time between collisions. The nematic order parameter responded more slowly, taking roughly $4000t_c$ to attain a stable value of $S \approx 0.7$, characteristic of the ordered phase. Following equilibration, a production run of length $75000t_c$ (over 5×10^6 collisions) was undertaken. During this period, order-parameter fluctuations of order $\pm 20\%$ occurred and the director remained almost constant in space, aligned with one of the simulation box axes. Configurations were written to tape for later analysis.

To determine the Frank constants, we used the procedure described earlier, based on Eqs. (4) and (5). We examined all wave vectors \mathbf{k} having components equal to 0, 1, or 2 times the minimum values commensurate with the box sides in each direction. The values at the origin, $E_{13}(0,0)$ and $E_{23}(0,0)$ were specified as zero rather than being obtained from the simulation [for a finite-size system the simulation values from Eqs. (4) and (5) would be finite, and expected to vanish as $V \rightarrow \infty$]. For all other values of k_1 and k_3 , E_{13} and E_{23} were calculated from run averages, and the statistical precision of each data point

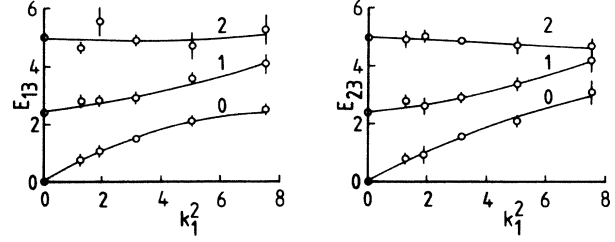


FIG. 1. Calculation of Frank elastic constants. We show sections through the surfaces $E_{13}(k_1^2, k_3^2)$ and $E_{23}(k_1^2, k_3^2)$. In each case we plot the data (points) and polynomial surface fits (lines) as functions of k_1^2 for fixed k_3 equal to 0, 1, 2 times the minimum k_3 possible in the simulation box.

estimated from the distribution of subrun averages. The points were correspondingly weighted in a least-squares-fitting routine which used a product of second-order polynomials in the variables k_1^2 and k_3^2 . The data, and sections through the fitted surface, are shown in Fig. 1. The low- k gradients are well defined, and the corresponding elastic constants are given in Table I. We report reduced elastic constants $K_i^* = K_i \sigma / k_B T$ where $\sigma^3 = 8ab^2$, T is the temperature, and k_B is Boltzmann's constant. The estimated precision of the final results is obtained by carrying out the above fitting procedure for each subrun independently, and assuming a normal distribution of the calculated elastic constants. For comparison, we give in Table I typical values of K_i^* (with σ estimated from the known approximate molecular dimensions), as measured experimentally for the nematogens N-(*p*-methoxybenzylidene)-*n*-butylaniline (MBBA) and para-azoxyanisole (PAA), which have similar axial ratios to the ellipsoids studied here.^{10,13} A detailed comparison would be pointless, in view of the highly idealized model employed here, but we note that our results are of the correct order of magnitude and in about the expected ratios, with $K_3(\text{bend}) > K_1(\text{splay}) > K_2(\text{twist})$. It would be interesting to compare these results with theoretical predictions. Unfortunately, there have been few calculations of this kind for ellipsoids. A density functional approach has been reported¹⁴ for the hard-body modification of the Gaussian overlap potential, which may be a close, but not exact, representation of hard ellipsoid overlap.¹⁵ Values read from Fig. 7 of Ref. 14 for the appropriate elongation and converted into reduced units have been included in

TABLE I. Elastic constants for ellipsoids. Given are $K_i^* = K_i \sigma / k_B T$ from molecular dynamics (estimated precision in parentheses), typical values from experiments on PAA and MBBA (with σ estimated from molecular dimensions), and the results of density functional theory (DFT) on a related model (taken from Ref. 14).

	K_1^*	K_2^*	K_3^*
MD	0.57 (0.03)	0.53 (0.04)	1.94 (0.09)
PAA	1.00	0.63	2.50
MBBA	1.10	0.68	1.60
DFT	0.65	0.33	1.23

Table I, and they are quite close to our simulation results. However, in these calculations a rather lower order parameter ($S=0.5$) and density (corresponding to $\rho \approx 0.61\rho_{cp}$), compared with our simulations, have been assumed, so these values are probably underestimates: The leading term is expected to be proportional to S^2 , and a comparison of K_i^*/S^2 values is much less encouraging.

The spherocylinder system was studied at several densities in the nematic region. An initial configuration of 576 aligned spherocylinders, at a density $\rho=0.45\rho_{cp}$, produced by Monte Carlo simulation, was allowed to equilibrate with the orientational constraint removed, and it formed a phase with order parameter $S \approx 0.33$. (Similarly equilibrated systems at lower densities all formed an isotropic fluid). Following this, a further molecular-dynamics equilibration run of length $2100t_c$ was carried out. This was followed by a production run of $5000t_c$. A higher density configuration, $\rho=0.5\rho_{cp}$, $S \approx 0.73$, was generated by uniform compression, followed by equilibration and production runs of similar length to the above, and the same procedure repeated to obtain data at $\rho=0.569\rho_{cp}$, $S \approx 0.91$. Further compression resulted in spontaneous ordering to form a stable smectic phase at $\rho \approx 0.6\rho_{cp}$. As in the ellipsoid case, the order parameters and director orientations remained nearly constant.

The calculation of Frank constants proceeded in the same way as that for ellipsoids. For the spherocylinder systems, the deficiencies of much shorter runs are partly offset by the greater range of small k vectors accessible in the larger simulation box. We used the lowest 15 accessible k_1 values. Along the 3-direction, however, the choice was very limited by incipient smectic ordering at the higher densities. A peak develops in the structure factor at $k_3=3$ times the minimum commensurate with the box, and we considered only k_3 values less than this in the fitting routine. This, in turn, affects the precision with which we can determine K_3 , and the confidence we may place in the results for this quantity. The fitting process was identical to that employed for ellipsoids, except that a linear functional form was adopted in the k_3^2 variable. The results in reduced units $K_i^* = K_i D/k_B T$ are summarized in Table II. Values of K_i^*/S^2 are plotted as func-

TABLE II. Elastic constants for spherocylinders. $K_i^* = K_i D/k_B T$ from molecular dynamics (estimated precision in parentheses) at three densities.

ρ/ρ_{cp}	K_1^*	K_2^*	K_3^*
0.450	0.05 (0.009)	0.04 (0.008)	0.07 (0.01)
0.500	0.37 (0.11)	0.26 (0.03)	0.49 (0.05)
0.569	2.06 (0.26)	1.00 (0.09)	0.67 (0.14)

tions of S and compared with theoretical predictions^{16,17} in Fig. 2. (No agreement between theory and simulation can be obtained by comparing states of the same density.) It can be seen that all the elastic constants increase dramatically with increasing density (and S), and, if anything, the growth in K_1 is more pronounced than that in K_2 and K_3 . There is at best moderate agreement between theory and simulation for K_1 and K_2 . For K_3 , the situation is worse: We do not see the expected rise, much more rapid than S^2 , that is predicted as S increases. We recall, however, that our K_3 values are the most suspect, due to the limitations mentioned earlier. We should also mention that the very low values of all the elastic constants at $\rho/\rho_{cp}=0.45$ are consistent with this state point being very close to the isotropic-nematic transition: Indeed, much longer simulation runs might reveal the nematic phase to be only metastable at this density.

The nematic-smectic transition occurs quite close to the highest-density studied here. If the nematic-smectic transition is a continuous one, as seems likely given the high degree of nematic ordering at this density, K_2 and K_3 should diverge while K_1 remains well behaved. We cannot see this in our results. Quite possibly the "critical" divergence of K_2 and K_3 is inhibited in a simulation box of this size as the relevant correlation lengths become large approaching the phase transition. It is not surprising, though, that we see a general increase in orientational rigidity of the system. The most dramatic effect we observe is in K_1 , and this may be due to the increased importance of coupling between splay deformations and density fluctuations in this tightly packed system.¹⁸

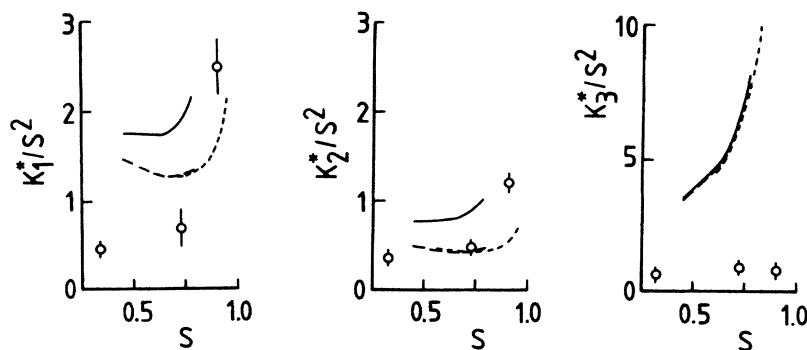


FIG. 2. Frank elastic constants for spherocylinders. We plot K_1^*/S^2 , K_2^*/S^2 , and K_3^*/S^2 as functions of S and compare with theoretical predictions in the same reduced units based on data from the following: Ref. 16, $L/D=5$ (solid line); Ref. 16, $L/D=\infty$ (long dashes); Ref. 17, $L/D=\infty$ (short dashes).

In conclusion, we have calculated by computer simulation, for the first time, the Frank elastic constants of nematic liquid-crystal phases with rotational and translational degrees of freedom. The results are encouraging, in that the simple hard ellipsoid and spherocylinder models give elastic constants of the correct order of magnitude and in the expected ratios. There are some caveats however. The tendency of the director to align with the simulation box axes suggests that periodic boundary conditions play some role in the formation of the ordered phase. Further simulations, using different system sizes and boundary conditions, are in progress to test this. For spherocylinders, in view of the run lengths employed, our results must be regarded as preliminary. We observe that the elastic constants increase with density. However, we cannot claim to see critical divergence near the nematic-smectic transition: This could only be observed for system sizes large compared with the smectic correlation length. This does not prevent us from comparing our results with theories which also neglect such pretransitional behavior. It seems that thus far density functional theories are only moderately successful at predicting elastic constants. In

view of the prediction that hard repulsive interactions and attractive forces both contribute significantly to the values of elastic constants,^{19,20} detailed comparison with experiment is premature. Nonetheless, there is every possibility of extending computer simulations to more realistic interaction models. It is clear that calculation of elastic constants with an accuracy comparable to experimental measurements (5–10%) requires rather long runs (of order $10^4 t_c$) and large system sizes (of order 10^3 molecules), but that this is within the capacity of current supercomputers.

Computer time for this study was made available on the CYBER-205 computers at the Universities of Manchester and Amsterdam. This work was funded by the Science and Engineering Research Council. The work of one of us (D.F.) was performed as part of the research program of the Stichting Fundamenteel Onderzoek der Materie (FOM) with financial support from the Nederlandse Organisatie voor Zuiver Wetenschappelijk Onderzoek (ZWO).

¹D. Frenkel and R. Eppenga, *Phys. Rev. Lett.* **49**, 1089 (1982); R. Eppenga and D. Frenkel, *Mol. Phys.* **52**, 1303 (1984).

²D. Frenkel, B. M. Mulder, and J. P. McTague, *Phys. Rev. Lett.* **52**, 287 (1984).

³D. Frenkel and B. M. Mulder, *Mol. Phys.* **55**, 1171 (1985).

⁴A. Stroobants, H. N. W. Lekkerkerker, and D. Frenkel, *Phys. Rev. Lett.* **57**, 1452 (1986); and *Phys. Rev. A* **36**, 2929 (1987).

⁵D. Frenkel, *J. Phys. Chem.* (to be published).

⁶D. J. Adams, G. R. Luckhurst, and R. W. Phippen, *Mol. Phys.* **61**, 1575 (1987).

⁷M. P. Allen and D. Frenkel, *Phys. Rev. Lett.* **58**, 1748 (1987).

⁸D. W. Rebertus and K. M. Sando, *J. Chem. Phys.* **67**, 2585 (1977).

⁹C. Zannoni, in *Molecular Physics of Liquid Crystals*, edited by G. R. Luckhurst and G. W. Gray (Academic, New York, 1979).

¹⁰P. G. de Gennes, *The Physics of Liquid Crystals* (Clarendon, Oxford, 1974).

¹¹F. C. Frank, *Discuss. Faraday Soc.* **25**, 19 (1958).

¹²D. Forster, *Ann. Phys. (N.Y.)* **85**, 505 (1974).

¹³W. H. De Jeu, *Physical Properties of Liquid Crystalline Materials* (Gordon and Breach, New York, 1980), Chap. 6.

¹⁴Y. Singh and K. Singh, *Phys. Rev. A* **33**, 3481 (1986).

¹⁵V. R. Bethanabotla and W. Steele, *Mol. Phys.* **60**, 249 (1987).

¹⁶A. Poniewierski and J. Stecki, *Mol. Phys.* **38**, 1931 (1979).

¹⁷S. D. Lee and R. B. Meyer, *J. Chem. Phys.* **84**, 3443 (1986).

¹⁸R. B. Meyer, in *Polymer Liquid Crystals*, edited by A. Ciferri, W. R. Krigbaum, and R. B. Meyer (Academic, New York, 1982), Chap. 6.

¹⁹W. M. Gelbart and A. Ben-Shaul, *J. Chem. Phys.* **77**, 916 (1982).

²⁰K. Singh and Y. Singh, *Phys. Rev. A* **34**, 548 (1986).